COMPDYN 2025
10th ECCOMAS Thematic Conference on
Computational Methods in Structural Dynamics and Earthquake Engineering
M. Papadrakakis, M. Fragiadakis (eds.)
Rhodes Island, Greece, 15-18 June 2025

# ON THE MULTISCIPLINARY APPROACH FOR THE EVALUATION OF THE STRUCTURAL BEHAVIOUR OF HISTORIC CONSTRUCTIONS

**M. Zucca[1], M. Scamardo[2], E. Reccia[1], E. Vecchi[1], V. Pintus[1] and F. Stochino[1]**

[1] Department of Civil, Environmental Engineering and Architecture, University of Cagliari, Via Marengo 2, Cagliari, Italy
{marco.zucca2, emanuele.reccia, enrica.vecchi, valentina.pintus, flavio.stochino}@unica.it

[2]Department of Architecture, Built Environment and Construction Engineering, Politecnico di Milano
Piazza Leonardo da Vinci 32, Milano, Italy
manuele.scamardo@polimi.it

**Abstract**

*During the last decades, the scientific community has increasingly focused on evaluating the structural behavior of historic buildings. In fact, these constructions often exhibit a complex structural response due to their unique configuration and the generally poor mechanical properties of the materials, as most of them were built with unreinforced masonry. For these reasons, the accurate reconstruction of the geometry of these buildings is essential for properly assessing their structural response under both static and dynamic loads.*
*In this paper, the structural performance of some iconic historic constructions has been investigated through several detailed numerical analyses. In particular, various Finite Element Models have been implemented based on the geometry reconstruction obtained from comprehensive laser scanner surveys which can capture all the intrinsic irregularities characteristic of heritage buildings. Non-linear analyses have been carried out to evaluate potential collapse mechanisms, highlighting the most critical structural elements.*

**Keywords:** Historic Constructions, Structural Behaviour, Lase Scanner Surveys, Non-linear Analyses.

# 1 INTRODUCTION

The structural rehabilitation of historical constructions actually represents one of the most important civil engineering research topics**.** In particular, the growing interest in preserving historical unreinforced masonry (URM) constructions has led to the development of new structural analysis methods based on a multidisciplinary approach. A fundamental aspect influencing the assessment of historical buildings' structural performance is the accurate reconstruction of their geometry, especially regarding vaults, arches, and buttresses [1]. During the last few years, several approaches based on the application of laser scanners [2,3], Unmanned Aerial Vehicles (UAVs) [4] and terrestrial photogrammetry [5,6] have been used to reconstruct the complex geometries of historical buildings, considering the inherent irregularities of the main structural elements. It is important to highlight that most of these constructions were built in seismic-prone zones and were constructed using traditional URM with various construction techniques. Particularly, religious sites, such as churches, cathedrals, sanctuaries, monasteries, etc. represent an important portion of the heritage building stock and are characterized by high levels of vulnerability to earthquake actions [7-9]. Focusing on Italian masonry buildings, many suffered significant damages during recent earthquakes, such as the 2009 L'Aquila earthquake, where 170 out of 240 monuments experienced major damage or partial failures [10]. In fact, this type of construction typically features a complex structural configuration due to the presence of slender walls and the lack of stiffening floors. Another important aspect that influences the structural performance of historical buildings is the quality of the used materials and the possible presence of degradation phenomena which can significantly decrease the material mechanical properties.

In this paper, the structural behavior of two different case studies will be analyzed by implementing advanced Finite Element Models (FEMs) derived from the 3D point-cloud laser scanner geometry obtained from in-situ surveys. The first case study is related to a historical masonry sail vault characterized by a complex brick pattern and by a segmental shape. The second one examines the unloading-reloading process used to carry out the retrofitting interventions of the nave's columns of the Santa Maria di Collemaggio Basilica, performed during the post-2009 L'Aquila earthquake reconstruction. In particular, the first case focuses on examining the static behavior of the masonry vault through a construction stage analysis. This analysis aims to assess how the stresses acting on various parts of the vault evolve throughout the construction process, with the assumption that no formwork is used. A sensitivity analysis was performed to obtain the minimum masonry tensile strength which can allow the construction of the vault without the presence of formworks. In the second case, the complex unloading-reloading procedure of the nave's columns has been analyzed considering two different solutions: the one proposed during the design phase and the one proposed during the construction phase. The obtained results are compared with measurements acquired during the construction work.

# 2 MASONRY VAULT

The analyzed masonry vault is a typical sail vault of Cagliari (Italy) built in the second half of the 19th century [11] and located on the ground floor of a historical building in the city downtown. It is part of a structural system built with solid bricks and composed of four vaults, each of which has four arches and square pillars.

As shown in Figure 1, the vault is characterized by several brick arrangements and by a lowered shape, that is nearly flat in correspondence to the crown. Four boundary arches limit the plan dimensions that are 5.88 x 5.68 m; the arch's maximum rise is 1.48 m at the key bricks. The vault has a total thickness of 12 cm, except at the lower sections corresponding to the interfaces between the vault and the masonry columns, where the thickness increases to 24 cm.

Figure 1: The masonry vault.

The vault geometries were reconstructed through a laser scanner survey conducted with the Leica Laser Scanner HDS 7000 (Figure 2). Four scans were performed to capture the precise geometry of the vaults and the bricks pattern. The acquired geometric data was then integrated with the chromatic features obtained by a photogrammetric survey.

Figure 2: The vault geometry obtained from laser-scanner surveys.

The 3D point-cloud obtained from the laser scanner survey provided an accurate reconstruction of the vault geometry, which was used to generate contour-level curves [22]. These curves describe the comprehensive surface of the vault and provide information on where the brick arrangement changes are defined (Figure 3a). A set of 30 cm-spaced polylines, has been then used to reconstruct a NURBS (Non-Uniform Rational Basis-Splines) surface representing the vault (Figure 3b) through Rhinoceros software [12].

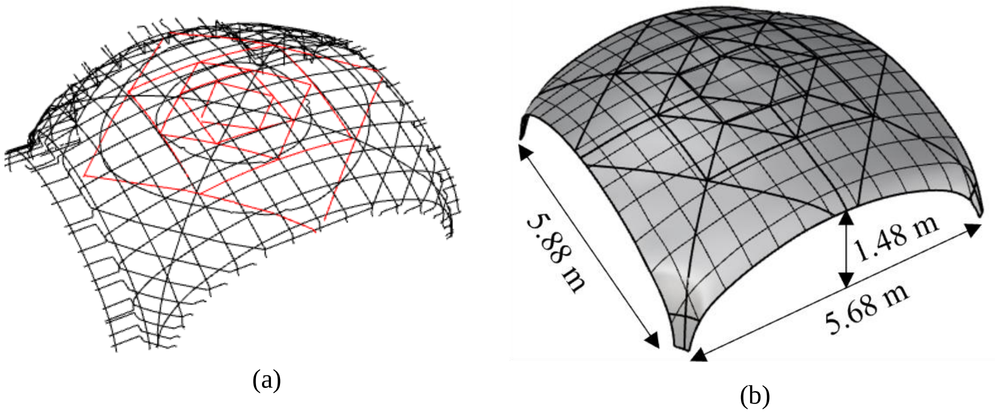


Figure 3: (a) Contour-level curves and (b) NURBS surface representing the vault.

To analyze the stress evolution on various parts of the vault during its construction process, an advanced 3D FEM has been implemented using the MIDAS FEA commercial software [13]. In particular, the FEM is made of 32670 six node triangular plate elements (having a maximum size of the mesh equal to 5 cm) while the four boundary arches are schematized using beam elements (Figure 4).

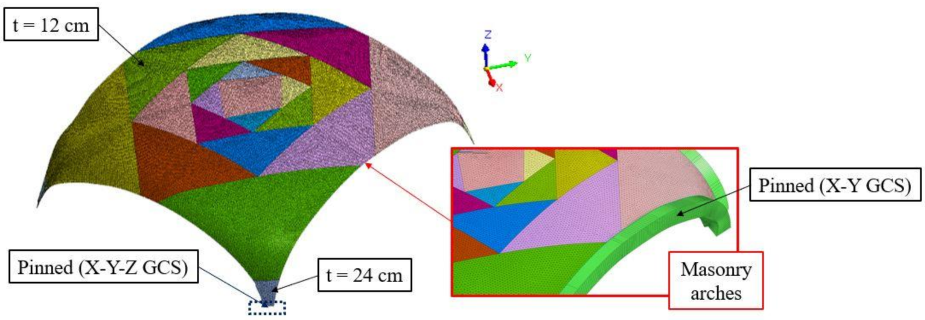


Figure 4: Vault FEM.

At the four boundary arches, simple supports acting along the horizontal direction have been used to simulate the presence of adjacent vaults and perimeter masonry walls, while both vertical and horizontal simple supports have been introduced at the interface between the vault and the masonry columns.

The main mechanical properties of the masonry are summarized in Table 1, where $\gamma$ is the unit weight, $E_1$ and $E_2$ are the Young modulus in the directions parallel and perpendicular to the bed joints, $\nu$ is the Poisson modulus, $G_{12}$ is the shear modulus in 1-2 plane, $G_{23}$ is the shear modulus in 2-3 plane and $G_{31}$ is the shear modulus in 3-1 plane.

| $\gamma$ | $E_1$ | $E_2$ | $\nu$ | $G_{12}$ | $G_{23}$ | $G_{31}$ |
|---|---|---|---|---|---|---|
| [kN/m$^3$] | [MPa] | [MPa] | [-] | [MPa] | [MPa] | [MPa] |
| 18 | 1450 | 1000 | 0.1 | 545 | 272.5 | 272.5 |

Table 1: Masonry primary mechanical properties.

The masonry orthotopic behavior has been accounted for using a series of local coordinate systems associated with the different brick arrangements (Figure 5).

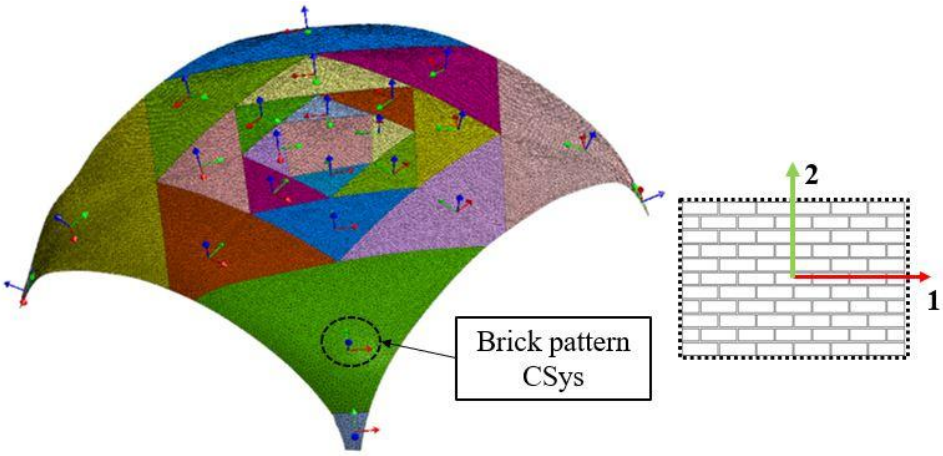


Figure 5: Local coordinate systems.

To assess the evolution in stresses affecting various parts of the vault during its construction process, a construction stage analysis was performed, considering the seven phases reported in Figure 6.

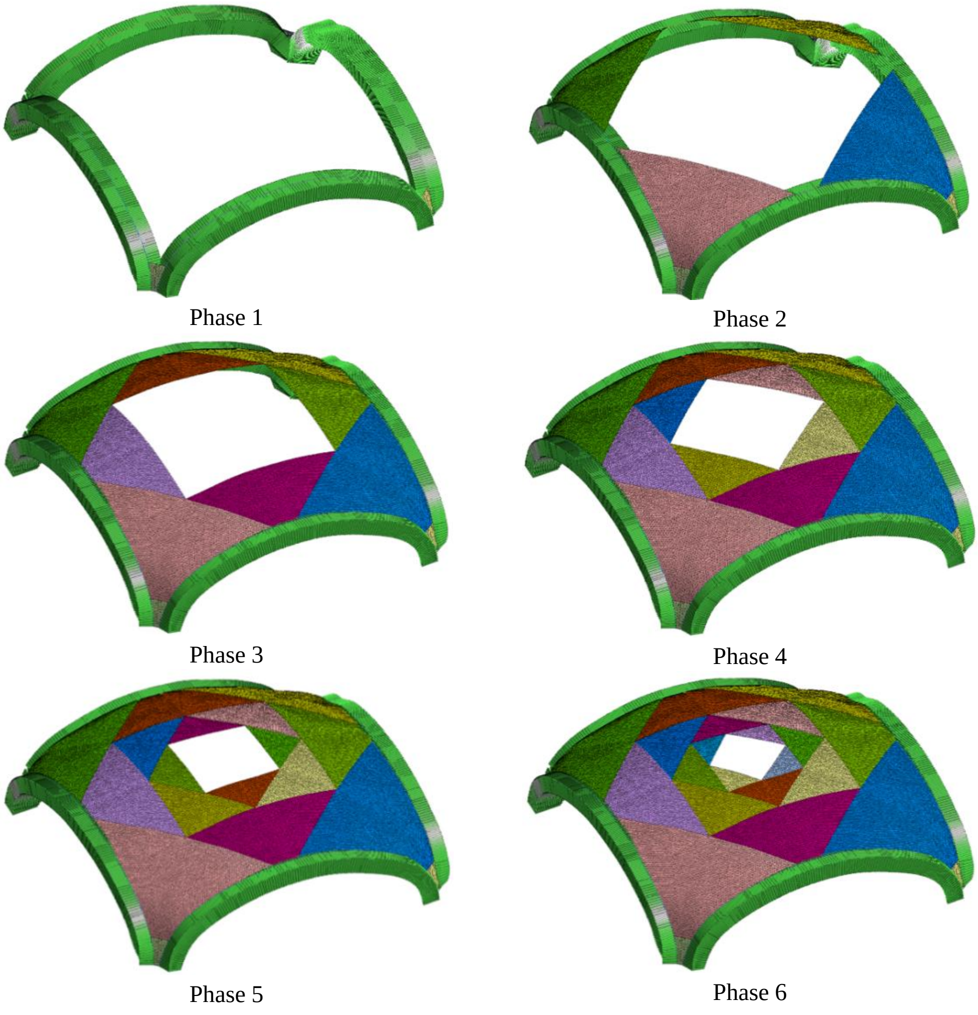

Phase 7

Figure 6: Vault construction phases.

The construction process has been developed starting from the presence of the four boundary arches (phase 1), following the different brick arrangements (phases 2-7) without the use of formworks.

The analysis results show that the first construction phases (phases 1, 2, 3, and 4) are characterized by low vertical displacements, which do not exceed 2.00 mm, while the increment of the vertical displacement appears almost constant during phases 5, 6, and 7. The maximum vertical displacement at the end of the vault construction (phase 7) is 3.56 mm, occurring at the vault crown. The final trend of the vertical displacement appears slightly asymmetric due to irregularities that characterize the vault's surface, arising from the asymmetry of the brick arrangements. The stress evolution is characterized by maximum tensile stress equal to 0.20 MPa localized at the key bricks of the boundary arches. This value of tensile stress occurs from the first construction phases. Conversely, the maximum value of compressive stress reached is 0.64 MPa, significantly increasing from phase 5.

To better understand how the construction process and various brick arrangements impact the results at the end of the construction stage analysis, a comparison between a standard static analysis with and without the different brick arrangement was performed. In this last case, the masonry has been considered as an isotropic material, having the following primary mechanical properties: Young modulus E = 1450 MPa, Poisson modulus ν = 0.1, and unit weight $\gamma = 18$ kN/m$^3$. Table 2 reports the results of this comparison in terms of vertical displacements ($T_z$), minor principal stresses (S-Major), and major principal stresses (S-Minor).

| | $T_z$ | S-Major | S-Minor |
|---|---|---|---|
| | [mm] | [MPa] | [MPa] |
| Construction stage analysis | 3.53 | 0.27 | 0.64 |
| Standard static analysis with brick arrangements | 1.84 | 0.14 | 0.33 |
| Standard static analysis without brick arrangements | 1.46 | 0.11 | 0.26 |

Table 2: Comparison of the results obtained from the different numerical analyses.

The maximum vertical displacement achieved through the standard static analysis is equal to 1.84 mm and 1.46 mm, with and without the inclusion of the different brick arrangement, respectively. These values are significantly lower than those calculated in phase 7 of the construction stage analysis. This discrepancy can be justified considering that, during the construction stage analysis, the effects of vertical displacements accumulate phase by phase, resulting in a larger effect, approximately twice the values obtained from the standard static analysis. The stress trend highlighted the fundamental role of the brick arrangements that influence mechanical behavior and the stress distribution along the vault surface. In particular, higher values of tensile stress are observed during the construction stage analysis of the vault. Indeed, the maximum value obtained through the standard static analysis is equal to 0.15 MPa regardless of the presence or absence of different brick arrangements.

Finally, a construction stage analysis was conducted based on the seven phases mentioned earlier, using a smeared cracking model [14,15] to evaluate the minimum value of masonry tensile strength required to build the vault without the use of formwork. A sensitivity analysis was performed considering masonry tensile strength values ranging from 0.30 MPa to 0.10 MPa. The obtained results confirmed that it is feasible to build the masonry vault without formwork only if the masonry has a tensile strength of at least 0.10 MPa. In fact, if the tensile strength is lower than 0.10 MPa, significant crack patterns begin to form from the initial phases of the construction, leading to the vault's collapse before the construction process is completed

## 3 UNLOADING AND RELOADING PROCESS OF THE NAVE'S COLUMNS

Santa Maria di Collemaggio Basilica was built in the late XIII century and represents an outstanding example of Romanesque architecture. Throughout its history, the Basilica has undergone various architectural and structural changes, often necessary due to the damage caused by seismic events [16,17]. The Basilica is characterized by the presence of three aisles with two lines of octagonal columns (Figure 7).

Figure 6: Santa Maria di Collemaggio Basilica.

The transept with two chapels and the choir is located on the opposite side of the façade. Two altars placed at the far ends of the transept and the stucco decoration of the walls, vaults, and chapels are a residual of the baroque decoration removed during the Seventies. The rest of the Basilica features bare walls with exposed wooden trusses to support a gable roof on the central nave and a pitched roof over the aisles.

During the 2009 L'Aquila earthquake, the Basilica suffered serious damage as reported in [18,19]. Some recent works described the main structural interventions that were realized during the reconstruction and retrofitting process [17,20].

According to historians, the stone masonry columns of the central nave are characterized by significant historical and artistic value. The two colonnades, composed of 14 columns, show several irregularities such as vertical and horizontal misalignments, different arch spans, inhomogeneous column heights, and diameters. For this reason, to accurately reconstruct this complex geometry, a precise laser scanner survey was performed. The average cross-section diameter of the columns is 115 cm for the shaft and 140-160 cm (top-bottom) for the base. The columns are approximately 4 m high, without considering the capital and the base, whose average heights are respectively 0.54 m and 0.81 m. The basement and the capital are made of a local limestone rock called *'breccia aquilana'*. As highlighted in [16], the columns have a good transversal displacement capacity due to the high compressive strength of the stone blocks ($f_m$ = 66.68 MPa) and the moderate level of dimensionless gravity axial load which leads to a ductile moment-curvature response of the cross-section [21]. However, material degradation and the presence of various construction defects negatively impact structural behavior. These defects include: (i) ineffective interlocking of stone blocks due to vertical alignment of head joints, (ii) an incoherent/rubble inner core, (iii) a non-uniform vertical stress field over the cross-section caused by previous block replacements, (iv) presence of damaged masonry units, and (v) the heterogeneous material properties of the blocks resulting from repair activities.

The post-2009 L'Aquila earthquake survey revealed that the central columns of both colonnades were significantly more damaged compared to the external ones. As shown in Figure 7, different types of damage have been identified during the survey, in particular: (i) the relative sliding of adjacent ashlars, (ii) the local crushing/spalling of blocks and the opening of pre-existent cracks, (iii) the presence of vertical cracks due to excessive compression stress, and (iv) the toe compression failure at the base of the columns.

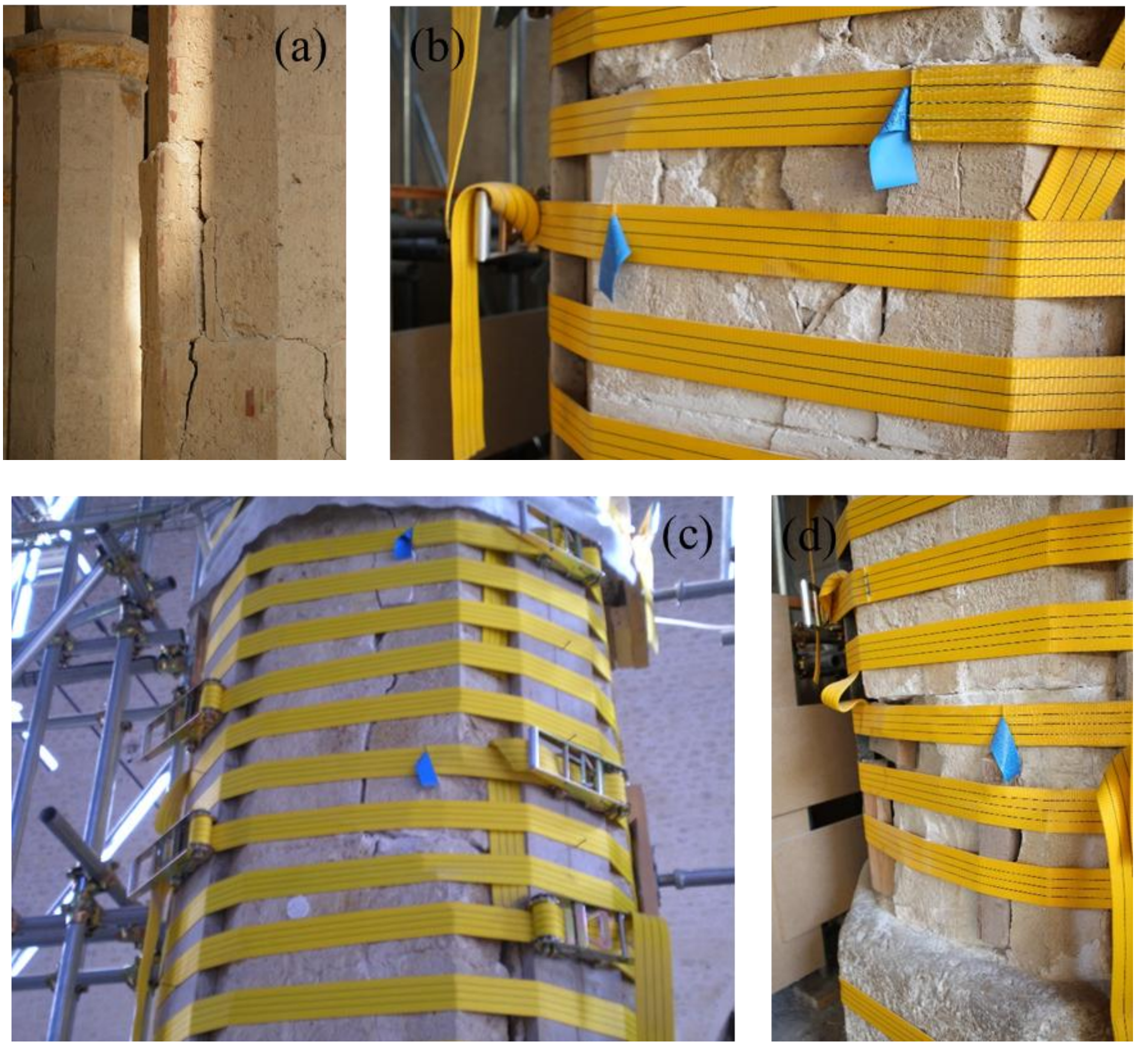


Figure 7: Damage observed during the post 2009 L'Aquila earthquake survey: (a) ashlars sliding, (b) crushing/ spalling, (c) vertical cracks and (d) toe compression failure.

Figure 8 reports the Basilica longitudinal section and the grouping of different columns according to their damage level. It is important to note that the columns adjacent to the collapsed transept (the undamaged columns, indicated in blue) were rebuilt using a reinforced concrete core in the 1970s and this is the reason why they did not suffer any seismic damage during the earthquake in 2009.

In light of the different types of damage observed, two repair techniques have been proposed:

- the central columns (heavily damaged) were completely disassembled and rebuilt using a combination of new blocks and original undamaged ashlars. In particular, the damaged blocks were replaced with new elements made of *'breccia aquilana'*. In addition, the inner part of the column, originally made of rubble masonry, was replaced with a new core of high-strength lime mortar. In specific situations with consistently large inner cores, regular stone blocks were also used to fill the center of the column;
- the lateral columns underwent localized block replacements and mortar injections, avoiding the complete disassembling of the elements.

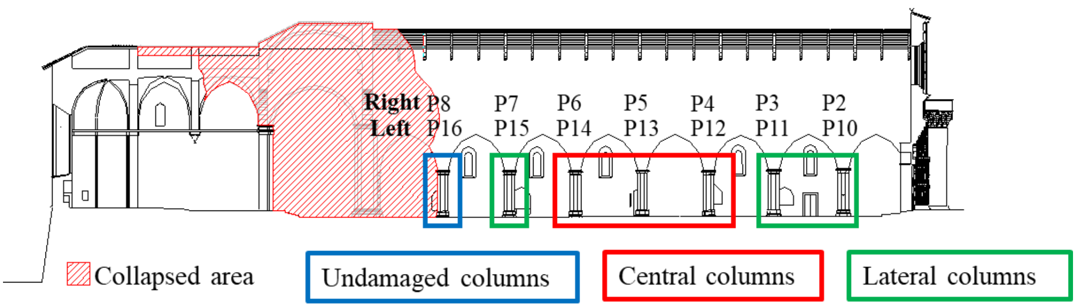

Figure 8: Basilica longitudinal section.

To perform the necessary repair interventions, the nave's columns underwent an unloading-reloading process. For this reason, a specific system was designed to transfer the vertical forces from the column to the ground. The designed system of frames sustained the arches and masonry walls during the execution of the interventions on the columns. Then, after the complete reloading of the retrofitted columns, the frame system was removed. During the analysis, a key aspect was ensuring the unloading process was not causing any damage to the masonry nave walls.

Two different unloading solutions were designed. The first one was based on the use of three steel ribs with frames that directly support the arches (Figure 9a). In this scenario, two columns can be unloaded and repaired simultaneously. The second solution acts on the abutments of the arches through a clamping system (Figure 9b).

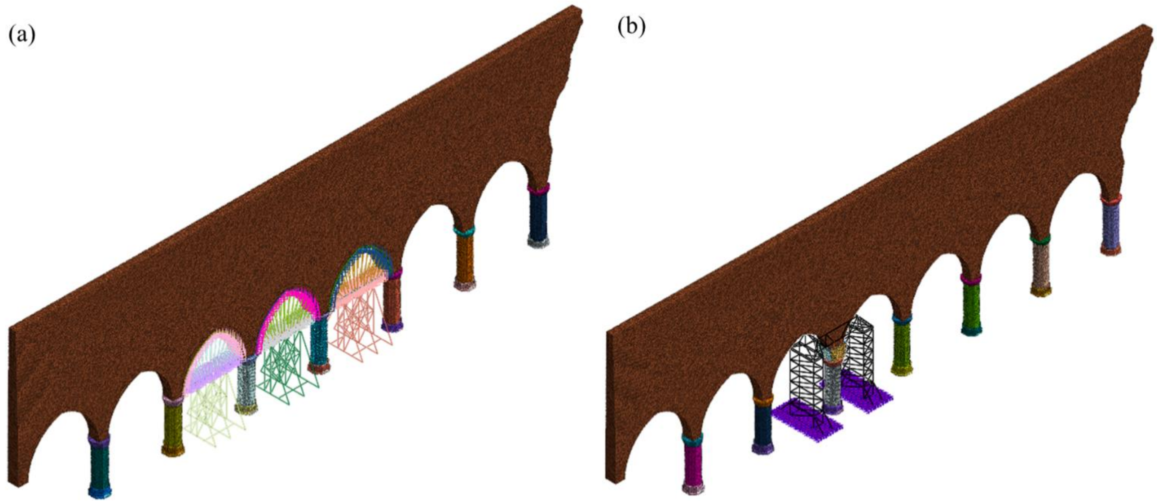

Figure 9: (a) steel ribs + frames system, (b) camping system.

To evaluate the feasibility of the proposed systems, a non-linear construction stage analysis, simulating all the different phases of the columns unloading-reloading process, was performed using MIDAS FEA commercial software [13]. Considering that the intervention only concerns the nave walls, a partial 3D finite element model representing the left nave was developed based on the 3D point-cloud obtained from the laser scanner survey. The remaining portion of the Basilica was considered by applying proper boundary conditions. In particular, one end of the nave wall was connected to the façade, while the other end was completely free due to the collapse of the transept area. The considered boundary conditions were the following: (i) fully-constrained ends at the bottom basements of the columns, (ii) transversal supports along the wall edge connected to the façade, and (iii) horizontal simple supports applied at the upper edge of the nave wall to reproduce the out-of-plane restraining effect of the roof. Furthermore, a uniform vertical pressure, equal to 26 kN/m$^2$, was applied to the upper edge of the nave wall.

The non-linear behavior of the masonry (stone and rubble) was modeled using the smeared cracking model [14,15]. Two materials were implemented in the FEM: stone masonry made of *'breccia aquilana'* ashlars for the outer portions of the columns and the arches, and rubble masonry for the inner core of the columns and the nave walls. Table 3 summarizes the main mechanical properties of the above-mentioned materials.

| Material | Unit Weight ($\gamma$) [kN/m$^3$] | Young Modulus (E) [N/mm$^2$] | Poisson Ratio ($\nu$) [-] | Compressive Strength ($f_m$) [MPa] |
|---|---|---|---|---|
| Stone masonry (*breccia aquilana*) | 25 | 20000 | 0.2 | 66.68 |
| Rubble masonry | 18 | 1600 | 0.2 | 2.00 |

Table 3: Main mechanical properties of stone and rubble masonry.

The following discusses the results obtained for the central column (third column from the façade) of the left aisle, one of the most damaged by the earthquake and interested by the complete disassembling and reconstruction. The main phases of the unloading-reloading process are outlined below (Figures 10 and 11):

- Phase 1. *Initial configuration.* The structure is modelled in its initial (post-earthquake) configuration, where the only load applied is the self-weight of masonry elements and roof. Three sub-stages are used to reproduce the historical construction sequence: (i) realization of the columns; (ii) building of the stone arches between the columns; (iii) realization of the nave walls on top of the arches.
- Phase 2. *Assembling of the supporting frame.* In the case of the struts-ribs system: (i) positioning of the steel frames along three adjacent arches; (ii) installation of six hydraulic jacks on top of each steel frame; (iii) positioning of the struts-ribs structures on top of the jacks; (iv) installation of wooden planks between the ribs and the stone masonry arches. For the clamping system: (i) positioning of the clamp around the arch abutment and mortar filling. The self-weight of the elements together with the compression loads of the pre-stressing bars are introduced, without altering the boundary conditions; (ii) installation of the steel frame (no connection with the clamp). For both solutions, the steel frames are located on a temporary foundation of wood joists and sand that protects the Basilica's pavement, represented in the FE models with an equivalent stiffness surface of springs.
- Phase 3. *Unloading phase.* The vertical load on the column is progressively transferred to the provisional steel frame by means of hydraulic jacks. In the struts-ribs system, the loads are transferred to the top HEB300 couple of horizontal beams. In the clamping solution, the loads are transferred from the vertical threaded bars to the horizontal trussed beam. From a numerical point of view, the unloading condition is reached when the sum of the vertical reactions at the base of the column is equal to the self-weight of the column.
- Phase 4. *Dismantling of the column*. Once the column is completely unloaded, the mortar joint between the capital and the abutment is removed and the disassembling of the column may begin. From a practical point of view, the mortar joint between the top of the capital and the abutment is cut away by a diamond wire sawing. The unloaded column is then separated from the upper part of the structure, allowing the execution of the retrofitting works. This was translated into the FE model by eliminating a thin layer of finite elements (100 mm) above the column's capital.
- Phase 5. *Repairing works*. The retrofitted column is re-introduced into the FE model through a new set of elements with updated mechanical properties of the inner core (Young modulus, $E = 15000$ N/mm$^2$, unit weight, $\gamma = 18$ kN/m$^3$, compressive strength $f_m = 40$ MPa and tensile strength $f_{tm} = 0.4$ MPa).

Phase 6. *Reloading phase.* After the intervention, the column is reloaded by the progressive unloading of the hydraulic jacks.

Phase 7. *Dismantling of the steel frame*. The last stage consists of removing the temporary supporting frames, together with the clamp and the mortar filling. By comparing the stress and displacement fields of Phase 1 and Phase 7, it is possible to quantify the effect of the construction process on the existing structure.

The results obtained from the construction stage analysis confirmed the feasibility of the proposed intervention procedures. Figure 12 shows the trend of the vertical base reactions of the columns during the unloading-reloading process applied to the central column (P12). It is important to highlight that the curve of the steel frame represents the total reactions of the three steel frames simultaneously in use divided by two to provide a comparable value "per column".

The reactions calculated at the base of the columns adjacent to the unloaded one decreased, especially when applying the strut-ribs system. Moreover, this phenomenon did not occur in columns far from the P12 column.

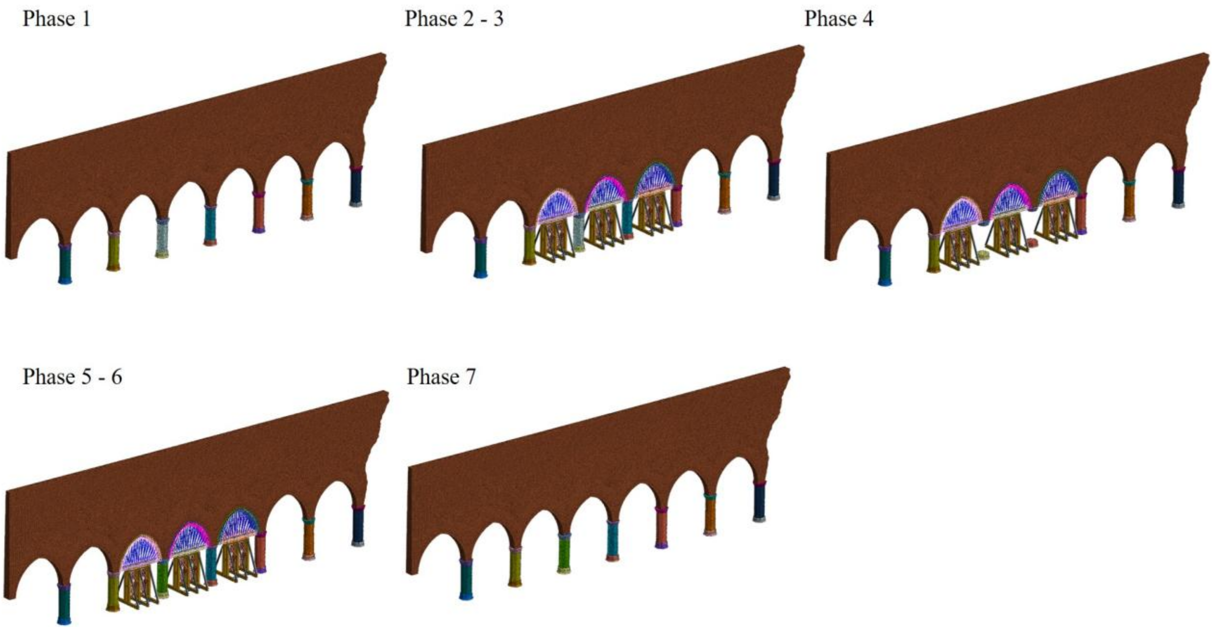


Figure 10: Unloading-reloading process for the steel ribs + frames system.

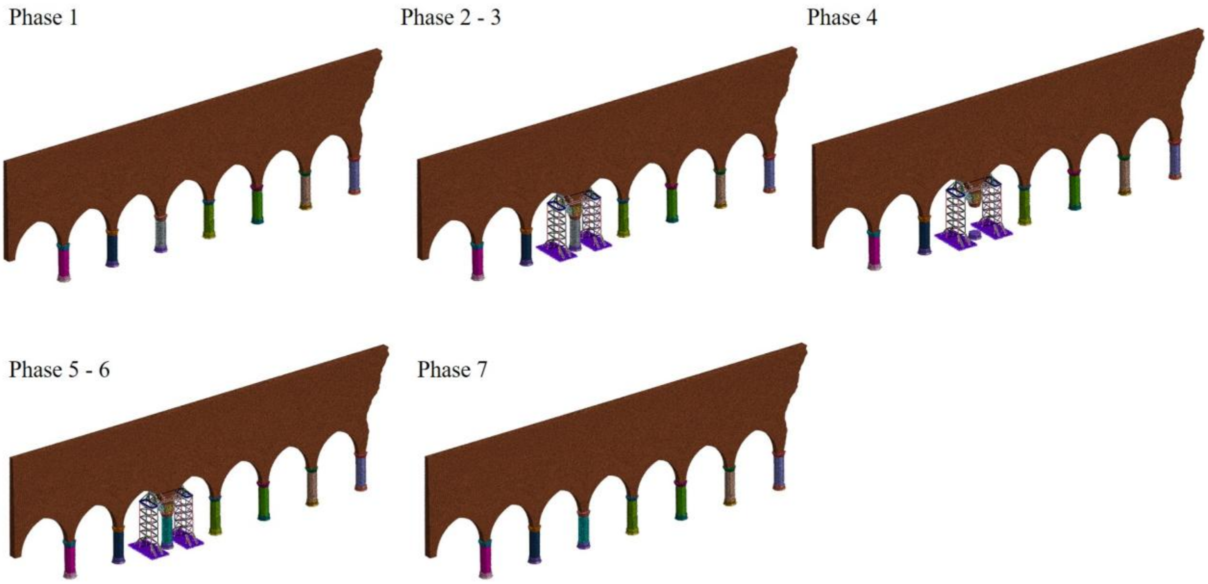


Figure 11: Unloading-reloading process for the clamping system.

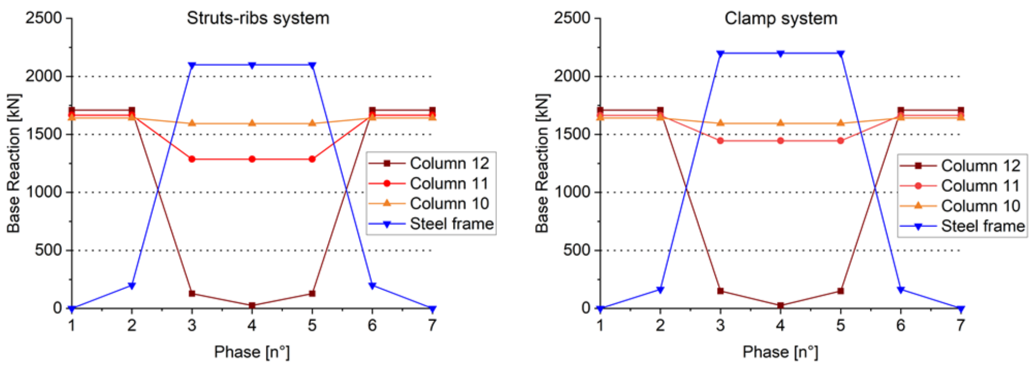


Figure 12: Trend of the column's base reactions during the proposed intervention procedures.

The stress levels obtained do not exceed the materials' strength limits. In fact, the maximum tensile stress acting on the stone masonry material of arches and abutments is about 1.5 MPa for the struts-ribs system and 1.3 MPa for the clamped solution. These values are lower than the tensile strength of the stone blocks, estimated to be the 10% of the compressive strength (6.7 MPa).

Considering the upper portion of the nave wall, realized using rubble masonry, the maximum tensile stress obtained is equal to 0.1 MPa and 0.12 MPa for the struts-ribs system and clamped system, respectively. Also in this case, the values are lower than the tensile strength of the material, assumed as 0.2 MPa.

The results indicate that both procedures are valid solutions for addressing the historical masonry columns of the Basilica. However, due to operational reasons, the clamping system was adopted during the retrofitting intervention of the Basilica. On site, the clamping steel frame was equipped with a set of transducers in order to monitor the real behavior of the system during the different phases of the unloading-reloading process. Figure 13 reports a comparison between the results obtained from the numerical model and the on-site measurements in terms of vertical displacement evaluated at the midpoint of the horizontal truss of the steel frame. Five load sub-steps were implemented in the numerical model, corresponding to the actual load steps used to reach the complete unloading of column P12 through the hydraulic jacks. The average error obtained was about 3%.

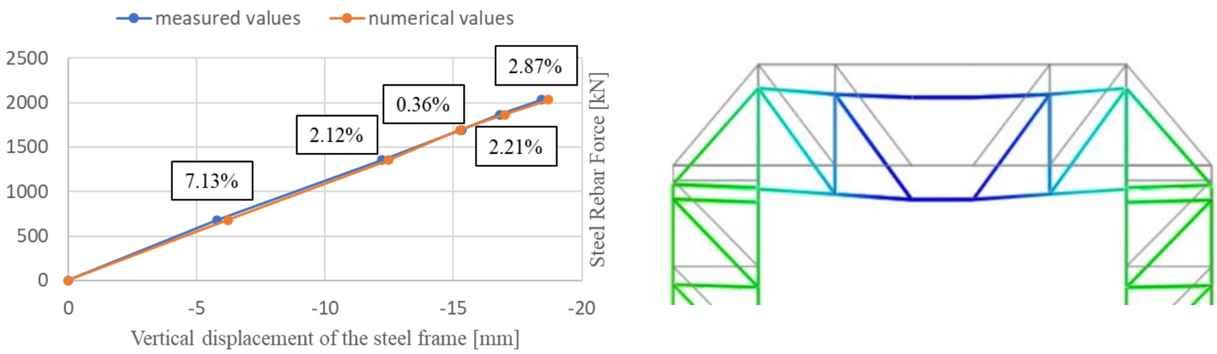


Figure 13: Comparison between the results obtained by the numerical model and the on-site measurements.

## 4 CONCLUSIONS

This paper highlights the importance of using a multidisciplinary approach for the correct evaluation of historical constructions' structural behavior. Two case studies were analyzed in detail: (i) the structural behavior of a historical masonry sail vault featuring a complex brick pattern and a segmental shape, and (ii) the feasibility of the unloading-reloading system used to conduct the retrofitting interventions on the nave's columns of Santa Maria di Collemaggio Basilica, during the post-2009 L'Aquila earthquake reconstruction. The following remarks can be noted:

- *Masonry vault*: using 3D modelling software, a NURBS surface representing the vault was reconstructed based on the 3D point cloud from the laser scanner survey. A Finite element model was implemented, and a construction stage analysis was performed to simulate the vault's construction process, assessing the evolution of the stresses acting upon different parts of the vault. The results of the construction stage analysis were compared with those obtained from a standard static analysis considering the presence or absence of the different brick arrangements, to assess the impact of the construction process. It is possible to highlight that the maximum value of vertical displacement obtained at the end of the construction stage analysis is approximately twice the one resulting from the standard static analysis, regardless of the presence or absence of the different brick arrangements. A significant difference in the trend of vertical displacement and the principal stress can also be observed. A sensitivity analysis was carried out in order to determine the minimum tensile strength required for the masonry to build the vault without the need for formwork. Adopting a smeared cracking model and considering a range of masonry tensile strength between 0.30 MPa and 0.10 MPa, the evolution of crack patterns throughout the various construction phases was analyzed. The results highlight that for values of masonry tensile strength below 0.10 MPa, constructing the vault without formwork is not feasible.

- *Columns unloading-reloading process*: considering the case study of the Basilica di Collemaggio, two different solutions to perform the unloading-reloading of the nave's masonry columns were analyzed. The first system (struts-ribs) was designed to unload two central columns within three adjacent arches by directly pushing on the arches' intrados with a system of struts and ribs. The second system (clamping system) operates on a single column by supporting the abutment of the arches with a post-tensioned steel clamp placed around the abutment section of the arches. The feasibility of these two solutions was investigated by implementing a nonlinear FE construction stage analysis reproducing the entire unloading-reloading process. The numerical results confirm the validity of both the proposed solutions. In fact, despite the change in the stress state generated by the unloading-reloading procedure, it remains within the material's strength limits. Additionally, the in-situ measurements collected during the implementation of the clamping system demonstrate a strong agreement with the numerical predictions.

## REFERENCES

[1] E.T. Boothy, Analysis of masonry arches and vaults. *Progress in Structural Engineering and Materials*, **3**, 246-256, 2001.

[2] H.A Jafaar, X. Meng, A. Sowter, P. Bryan, New approach for monitoring historic and heritage buildings: Using terrestrial laser scanning and generalised Procrustes analysis. *Structural Control and Health Monitoring*, **24**, 2017.

[3] J. Balado, E. Frias, S.M. Gonzalez-Collazo, L. Diaz-Vilarino, New Trends in Laser Scanning for Cultural Heritage. *Lecture Notes in Civil Engineering*, **258**, 167-186, 2022.

[4] T.D. Stek, Drones over Mediterranean landscapes. The potential of small UAV's (drones) for site detection and heritage management in archaeological survey projects: A case study from Le Pianelle in the Tappino Valley, Molise (Italy). *Journal of Cultural Heritage*, **22**, 1066-1071, 2016.

[5] K. Kinglsland, Comparative analysis of digital photogrammetry software for cultural heritage. *Digital Applications in Archaeology and Cultural Heritage*, **18**, e00157, 2020.

[6] P. Arias, J. Herraez, H. Lorenzo, C. Ordonez, Control of structural problems in cultural heritage monuments using close-range photogrammetry and computer methods. *Computers & Structures*, **83**, 1754-1766, 2005.

[7] S. Lagomarsino, S. Cattari, PERPETUATE guidelines for seismic performance-based assessment of cultural heritage masonry structures. *Bulletin of Earthquake Engineering*, **13**, 13-47, 2015.

[8] G. Milani, M. Valente, Comparative pushover and limit analyses on seven masonry churches damaged by the 2012 Emilia-Romagna (Italy) seismic events: Possibilities of non-linear finite elements compared with pre-assigned failure mechanisms. *Engineering Failure Analysis*, **34**, 761-778, 2015.

[9] A. Jain, M. Acito, C. Chesi, Seismic sequence of 2016–17: Linear and non-linear interpretation models for evolution of damage in San Francesco church, Amatrice. *Engineering Structures*, **211**, 110418, 2020.

[10] G. Brandonisio, G. Lucibello, E. Mele, A. De Luca, Damage and performance evaluation of masonry churches in the 2009 L'Aquila earthquake. *Engineering Failure Analysis*, **34**, 693-714, 2013.

[11] D. Wendland, Traditional vault construction without formwork: masonry pattern and vault shape in the historical technical literature and in experimental studies. *International Journal of Architectural Heritage*, **1**, 311-365, 2007.

[12] Rhinoceros 7 user manual, Robert McNeel & Associates, 2020, www.rhino3d.com.

[13] Midas FEA Analysis Reference, 2022, www.midasuser.com.

[14] F.J. Vecchio, M.P. Collins, Compression response of cracked reinforced concrete. *ASCE Journal of Structural Engineering*, **119**, 3590-3610, 1993.

[15] M. Petrangeli, J. Ožbolt, Smeared Crack Approaches—Material Modeling. *ASCE Journal of Engineering Mechanics*, **122**, 545, 1996.

[16] P. Crespi, A. Franchi, N. Giordano, M. Scamardo, P. Ronca, Structural analysis of stone masonry columns of the Basilica S. Maria di Collemaggio. *Engineering Structures*, **129**, 81-90, 2016.

[17] M. Zucca, P. Crespi, N. Longarini, M. Scamardo, The new foundation system of the Basilica di Collemaggio's transept. *International Journal of Masonry Research and Innovation*, **5**, 67-84, 2020.

[18] V. Gattulli, E. Antonacci, F. Vestroni, Field observations and failure analysis of the Basilica S. Maria di Collemaggio after the 2009 L'Aquila earthquake. *Engineering Failure Analysis*, **34**, 715-734, 2013.

[19] R. Brumana, S. Della Torre, M. Previtali, L. Barazzetti, L. Cantini, D. Oreni, F. Banfi, Generative HBIM modelling to embody complexity (LOD, LOG, LOA, LOI): surveying, preservation, site intervention—the Basilica di Collemaggio (L'Aquila). *Applied Geomatics*, **10**, 545-567, 2018.

[20] N. Longarini, P. Crespi, M. Scamardo, Numerical approaches for cross-laminated timber roof structure optimization in seismic retrofitting of a historical masonry church. *Bulletin of Earthquake Engineering*, **18**, 487-512, 2020.

[21] N. Giordano, P. Crespi, A. Franchi, Flexural strength-ductility assessment of unreinforced masonry cross-sections: analytical expressions. *Engineering Structures*, **148**, 399-409, 2017.

[22] A. Cazzani, N. Grillanda, G. Milani, V. Pintus, E. Reccia, Structural Evaluation of Typical Historical Masonry Vaults of Cagliari: Sensitivity to Bricks Arrangements. 12th International Conference on Structural Analysis of Historical Constructions (SAHC), 29-30 September – 1 October 2021 (online).